

# Molecular-dynamics study of the melting of hexagonal and square lattices in two dimensions

L. L. Boyer\*

*Complex Systems Theory Branch, Naval Research Laboratory, Washington, D.C. 20375-5345*

(Received 11 August 1995)

Simple pair potentials are discussed which give hexagonal- and square-lattice ground states in two dimensions. Molecular-dynamics calculations for these potentials are used to study transitions between the two lattices and melting. The melting temperature is found to be a minimum near the point where the barrier between the two structures, as a function of lattice strain, is also a minimum.

## I. INTRODUCTION

One of the most basic properties to consider in the comparison of two- and three-dimensional (2D and 3D) systems is the structure of the ground state of a collection of identical particles. Some general differences are well known. For example, in 3D the ground-state structure at constant volume depends on the type of repulsive interaction:<sup>1</sup> Interactions of the form  $1/r^n$  favor close-packed structures for large  $n$  and more open structures for  $n \leq 7$ . On the other hand, the hexagonal (or triangular) lattice is always favored for such potentials in 2D.<sup>2-4</sup> More recently, Zabinska<sup>5</sup> has shown that the square lattice can never be stable for potentials with the form  $V(r) = A/r^n + B/r^m$ .

More general considerations also seem to favor the hexagonal lattice. One can show, from a Voronoi-construction definition of coordination number and a theorem due to Euler, that the average coordination number of a periodic 2D system is exactly six, that of the hexagonal lattice. This can be interpreted as suggesting, based on geometrical considerations alone, that sixfold coordination is special, and therefore, to be expected regardless of the interactions. On the other hand, this definition of coordination number can be physically unrealistic, e.g., an infinitesimal distortion of the square lattice is identified as sixfold coordinated by this definition.

For these reasons, and the fact that pair potentials applied thus far give hexagonal ground states, there seems to be a general perception that simple pair potentials necessarily produce hexagonal ground states in 2D. In this paper we demonstrate that this is not the case. A class of potentials is considered that can have either hexagonal- or square-lattice ground states depending on the value of a single adjustable parameter (Fig. 1). We then examine, using molecular-dynamics simulation with selected potentials, transitions between the two structures, and consider the influence of the variations in the potential on the melting temperature.

## II. THE POTENTIAL

Consider a monatomic lattice in two dimensions with nearest-neighbor separation  $r_0$ . The hexagonal lattice has six nearest neighbors, while the square lattice has only four. However, the square lattice has its four next-nearest neighbors relatively nearer than the next-nearest neighbors of the hexagonal lattice;  $\sqrt{2}r_0$  compared to  $\sqrt{3}r_0$ . This suggests that

one can stabilize the square lattice if the second neighbors of the square lattice are brought into the range of the potential without including the second neighbors of the hexagonal lattice. Ladd and Hoover<sup>6</sup> noted this could be achieved by applying pressure to particles interacting with piecewise Hooke's law potentials. In general, a potential which is just wide enough to lower the energy substantially from the second-nearest-neighbor interactions of a square lattice, but not so wide as to achieve the same for a hexagonal lattice, can be expected to produce a square-lattice ground state. Such a potential can be effectively modeled by the sum of two Gaussians and a  $1/r^{12}$  term for repulsion at short range:

$$V(r) = a/r^{12} - c_1 \exp[-b_1(r-r_1)^2] - c_2 \exp[-b_2(r-r_2)^2]. \quad (1)$$

To optimize the conditions for producing a square-lattice ground state  $r_2/r_1$  should be approximately  $\sqrt{2}$ , the coefficients of the Gaussian terms should be approximately equal and their widths should be about half  $r_2 - r_1$ . The  $a/r^{12}$  term provides a hard repulsive interaction, but it should not dominate except for  $r < r_1$ . We choose  $r_1 = 1$ ,  $c_1/a = 2$ ,  $b_1 = b_2 = 8$ ,

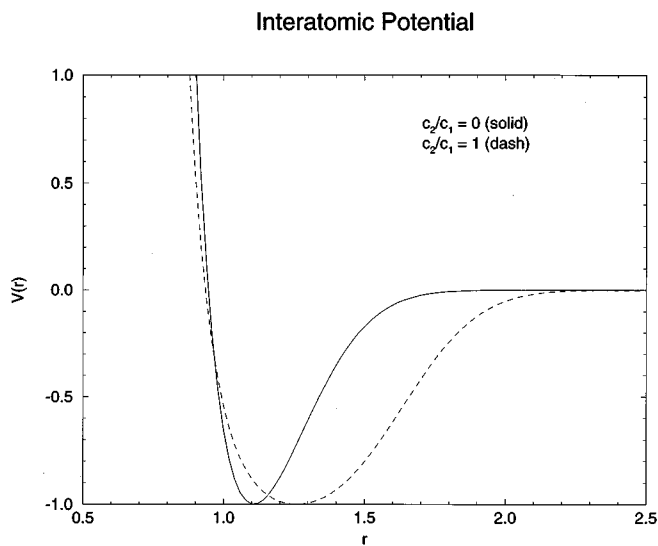


FIG. 1. The pair potential [Eq. (1)] with parameters as given in the text and  $c_2/c_1 = 0$  (solid curve, hexagonal-lattice ground state) and  $c_2/c_1 = 1$  (dashed curve, square-lattice ground state).

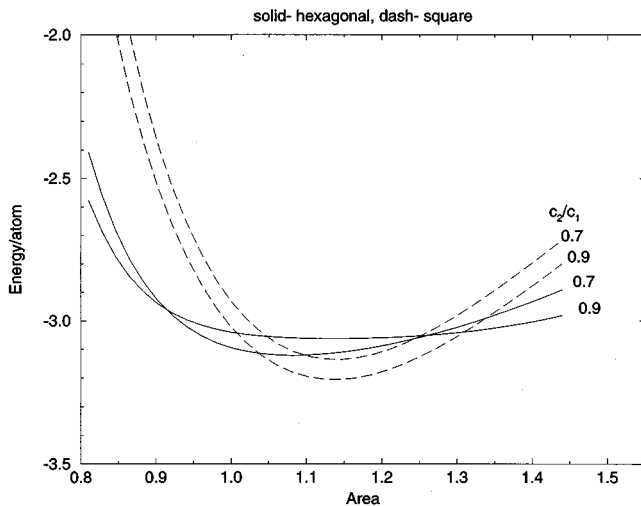


FIG. 2. Energy of the hexagonal (solid curves) and square (dashed curves) lattices as a function of the unit-cell area for potentials with  $c_2/c_1=0.7$  and  $0.9$ .

and scale  $V(r)$  so its minimum value is  $-1$ . At this point one could change  $V(r)$  gradually from producing hexagonal to square-lattice ground states by fixing  $c_2=c_1$  and varying  $r_2$  from 1 to approximately  $\sqrt{2}$ , or by fixing  $r_2$  and varying  $c_2/c_1$ . We choose the latter, with  $r_2=1.425$ , a value selected to give nearly the same equilibrium area in both hexagonal and square lattices when the equilibrium energies of the two lattices are nearly degenerate. Curves for  $V(r)$  with  $c_2=0$  and  $c_2/c_1=1$  are shown in Fig. 1.

The energy as a function of area for the two lattices is shown in Fig. 2 for two values of  $c_2/c_1$ :  $0.7$ , for which the two structures have nearly equal minima and  $0.9$ , for which the square lattice has substantially lower energy.

The change in the minimum energy from that of the hexagonal lattice is plotted as a function of shear strain for selected values of  $c_2/c_1$  in Fig. 3. If the hexagonal lattice is expanded by  $\sqrt{3}$  along any of three special directions (lines to

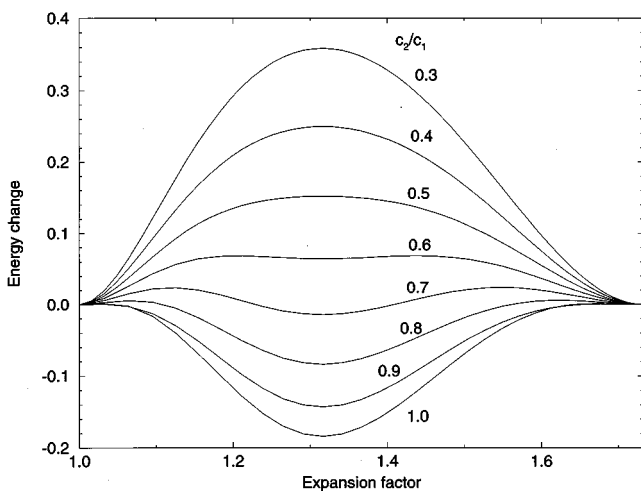


FIG. 3. Energy change from the hexagonal-lattice value as a function of expansion factor and minimized with respect to expansion direction and area/atom for the potentials with  $c_2/c_1=0.3, 0.4, \dots, 1.0$ . The extrema at  $\sim 1.3$  correspond to the square-lattice structure.

the nearest neighbors) keeping the area/atom fixed, then the strained lattice is again perfectly hexagonal. The curves in Fig. 3 were obtained by increasing the expansion factor from 1 to  $\sqrt{3}$  while minimizing the energy with respect to expansion direction and area/atom. For future reference, the energy change along such a curve will be called the minimum strain (MS) barrier. One could just as well plot these curves in terms of a strain which takes the square lattice into itself. Specifically, an expansion of  $(1 + \sqrt{5})/2$  along directions making the angles of  $\arctan[(1 + \sqrt{5})/2]$ , or  $\arctan[2/(1 + \sqrt{5})]$ , with respect to nearest-neighbor directions, transforms the square lattice into itself.<sup>7</sup>

### III. MOLECULAR-DYNAMICS RESULTS

In this section we examine the results of molecular-dynamics (MD) calculations obtained using  $V(r)$  (above) for selected values of  $c_2/c_1$  with  $r_2=1.425$ . We choose to carry out simulations on free clusters of atoms because solids without free surfaces can readily superheat above the melting temperature ( $T_m$ ), either in MD simulations using periodic boundary conditions, or in coated clusters, both experimentally,<sup>8</sup> and in MD simulation.<sup>9</sup> For convenience, the mass and Boltzmann's constant are taken to be unity. In these units the temperature for a 2D system is simply the average kinetic energy, or half the average velocity squared.

There is a vast literature dealing with the properties of melting in two dimensions. For a recent review, see Glaser and Clark.<sup>10</sup> Much of the work attempts to determine the precise nature of the transition, whether it is first order or continuous, and whether or not it is preceded by a transformation to a "hexatic" phase. Of course, all of the work deals with the melting of the hexagonal lattice. Here we are interested only in determining approximate values for the melting temperature as a function of the parameter that changes the system from one that melts from the hexagonal lattice to one that melts from the square lattice.

Clusters with approximately circular shape were prepared from the bulk minimum energy lattices. Small random displacements of the atoms were included at the beginning of the simulations to aid in thermalization. In a typical run the energy was increased by a small amount ( $\sim 0.01$ /atom) every  $\sim 10\,000$  time steps (step size of  $0.02$ ), by appropriately scaling the velocities, until the cluster had clearly melted. Melting was identified by the onset of diffusion. This was monitored by computing the average square of the displacement of atoms per unit time from their positions at some earlier time:

$$D^2 = \frac{1}{N(t-t_0)} \sum_{i=1}^N [r_i(t) - r_i(t_0)]^2. \quad (2)$$

Separate averages were taken over atoms which, at  $t_0$ , were within selected radii,  $R_j$ , with  $R_{j-1} < r_i(t_0) < R_j$ , to monitor diffusion in different parts of the cluster. Since each cluster was prepared without linear or angular momentum, and scaling the velocities does not change these quantities, any change in atomic positions over a long period of time either represents diffusion within the cluster or evaporation, which was independently monitored. Melting occurred before the onset of evaporation in clusters with  $c_2/c_1 > \sim 0.3$ . Values for

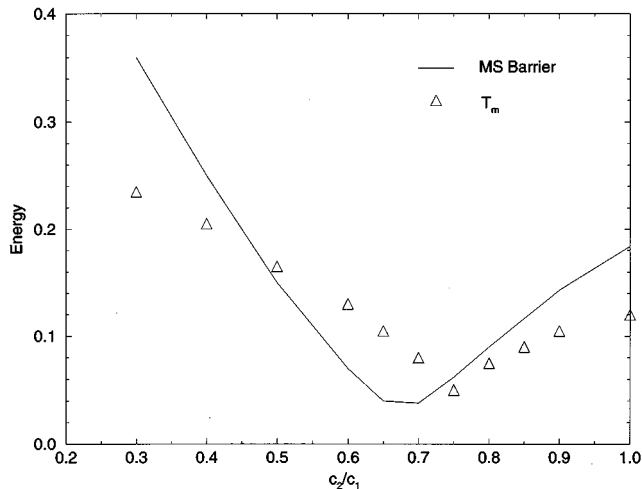


FIG. 4. Melting temperature (triangles) and MS barrier (solid curve) as a function of  $c_2/c_1$  for  $N \sim 200$  atom clusters.

$T_m$  were defined to correspond to the onset of diffusion in the innermost region of the clusters.

Results for  $T_m$ , obtained for  $N \sim 200$  atom clusters, are plotted in Fig. 4, along with the MS barriers, as a function of  $c_2/c_1$ . The  $T_m$  values are considered accurate to within  $\sim 10\%$ . While longer runs could improve this accuracy, the trend in Fig. 4 is clear:  $T_m$  decreases with increasing  $c_2/c_1$  to approximately the point where the MS barrier is minimum, and then increases beyond that point. The trend is the same for smaller ( $N \sim 100$ ) clusters, although the melting temperatures are generally smaller by  $\sim 15\%$ .

Simulations were carried out for decreasing as well as increasing energy. Melting (freezing) was found to be reversible in the sense that the temperature and diffusion as a function of energy,  $T(E)$  and  $D(E)$ , were essentially the same upon heating or cooling. Small nonlinear features in  $T(E)$  were apparent near the melting point, but these were not examined in detail. A better analysis of these features could be achieved by running for longer times on a finer energy mesh. However, our purpose was simply to identify an approximate value of  $T_m$ , and this was accomplished most easily from the onset of diffusion.

With the exception of the  $c_2/c_1 = 0.7$  and  $0.75$  cases (discussed separately below), the structure returned to that of its ground state after melting and refreezing. The precise after-freezing structures differed from the before-melted structures only in lattice orientations and minor shape changes.

The after-freezing structures for the  $c_2/c_1 = 0.75$  clusters showed some influence of the hexagonal lattice even though the square lattice is nearly  $0.05/\text{atom}$  lower in energy than the hexagonal lattice. A position plot of the structure obtained after reducing the temperature from  $T = 0.15$  (well above  $T_m$ ) to  $T \sim 0.01$  by removing energy at a rate of  $0.01$  per atom every 8192 time steps is shown in Fig. 5. The blackened areas are regions of space that were occupied by an atom in a sequence of, in this case, 8192 steps. Notice that the cluster has a single square-lattice domain with some distortions near the edges. However, the shape of the cluster is clearly not optimal. Another simulation at a two-times slower quench rate ( $0.005/\text{atom}/8192$  steps) produced a multidomain structure with both square and hexagonal regions

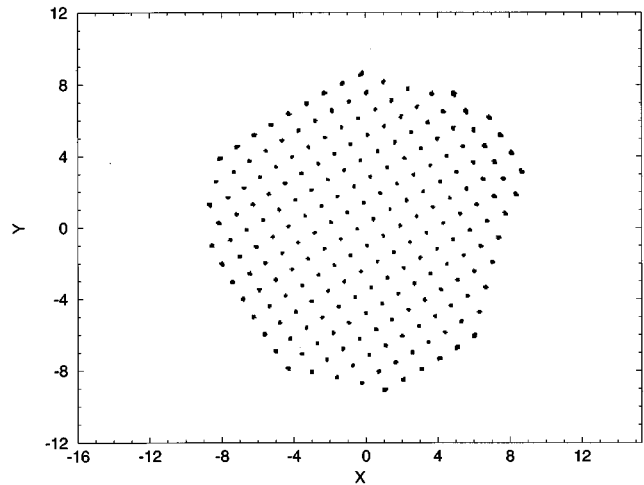


FIG. 5. Position plot for 8192 time steps of an  $N = 213$  cluster of atoms interacting with the  $c_2/c_1 = 0.75$  potential at  $T \sim 0.01$  after removing energy from the liquid at a rate of  $0.01/\text{atom}/8192$  steps.

with an overall shape which is nearly circular (Fig. 6). Apparently the longer run was sufficient to form a more favorably shaped surface, which involved both lattice types. The after-freezing structure of a larger cluster ( $N = 385$ ) was found to be a single-domain square lattice for both the above quench rates, consistent with the fact that surface effects are expected to be less important for larger clusters.

The  $c_2/c_1 = 0.7$  potential has nearly degenerate square- and hexagonal-lattice energies, with the square lattice winning by only  $0.015/\text{atom}$ . Thus, one would expect a stronger influence of the hexagonal structure in clusters with this potential, especially when considering the fact that the hexagonal lattice has lower energy for a wide range of areas (Fig. 2). Indeed, this was found to be the case. A qualitative difference was seen in the diffusion as a function of temperature compared to results obtained for the other potentials. Three cluster sizes were considered;  $N = 89, 213,$  and  $385$ . The  $N = 89$  atom clusters seemed to have three temperature ranges with qualitatively different diffusion characteristics:  $T < \sim 0.04$  where the diffusion was zero,  $\sim 0.04 < T < \sim 0.08$ ,

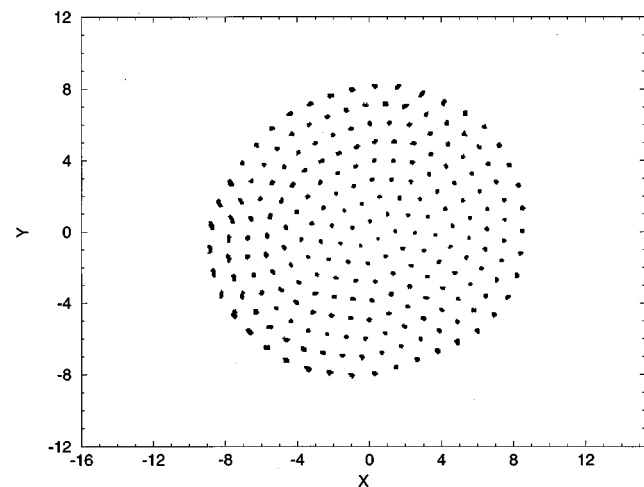


FIG. 6. Same as in Fig. 5 with half the quench rate ( $0.005/\text{atom}/8192$  steps).

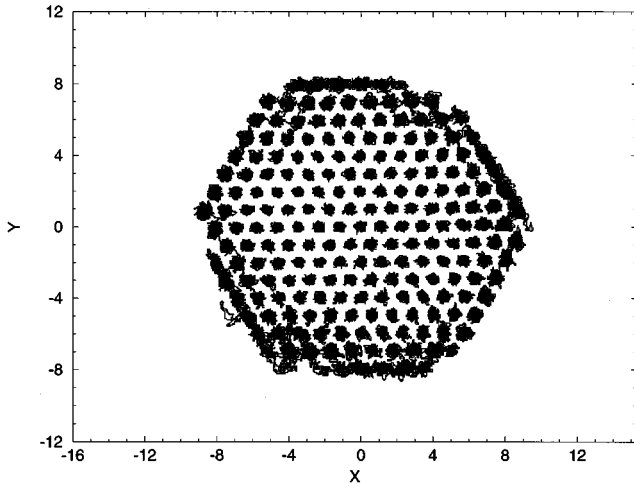


FIG. 7. Position plot for 8192 time steps of an  $N=199$ ,  $c_2/c_1=0.5$ , cluster at  $T=0.14$ , showing surface melting.

where there was clearly diffusion, but it was relatively low and increased at a qualitatively lower rate with increasing temperature than for  $T > \sim 0.08$ . The results for  $N=213$  were similar except the diffusion was much lower in the intermediate-temperature region. Calculations for the 385 atom cluster showed even lower, essentially zero, diffusion in this region. Additional analysis in this temperature range showed the structure had large predominately hexagonal regions which persisted for long periods of time, and these periods increased with increasing  $N$ . Thus we conclude that the  $c_2/c_1=0.7$  potential has a structural transformation from square to hexagonal with increasing temperature, at  $T \sim 0.04$ , before it melts at  $T \sim 0.08$ . Removing energy from the liquid state at the rate of 0.01/atom/8192 steps produced mixed-phase structures for the smaller clusters, similar to that shown in Fig. 6. However, the same quench rate applied to the  $N=385$  atom cluster produced a single-domain hexagonal structure at low temperatures ( $T < 0.04$ ).

Surface melting was observed in varying degrees for all clusters studied. This is illustrated in Figs. 7 and 8 with position plots for two clusters with hexagonal and square lattices just below their melting temperatures. Each covers a

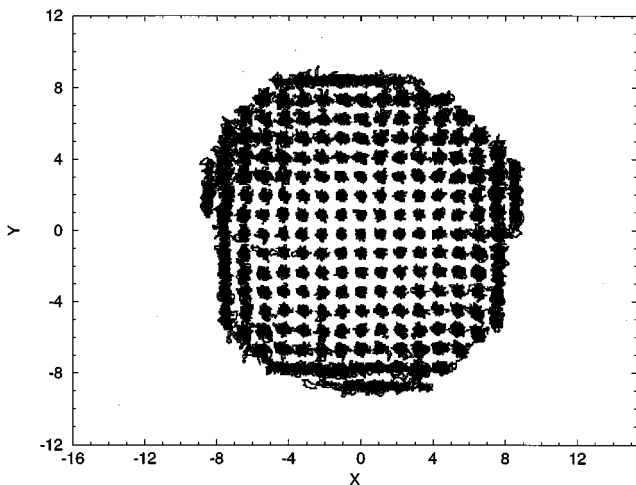


FIG. 8. Position plot for 8192 time steps of an  $N=213$ ,  $c_2/c_1=0.9$ , cluster at  $T=0.1$ , showing surface melting.

period of 8192 time steps. Above the melting temperature, plots covering the same time period show an almost completely blackened circular region.

#### IV. DISCUSSION

The approximate correlation between melting temperature and MS barrier, previously identified for 3D solids,<sup>11</sup> and now, for 2D solids as well (Fig. 4), suggests a general mechanism for melting: A solid melts when it acquires enough thermal energy to traverse the energy “landscape” associated with large lattice strain, or, more general types of shape change that, perhaps, could be described in terms of some sort of lattice defects.<sup>12</sup> Bear in mind, of course, that it is unrealistic to characterize the entire portion of the energy landscape that could be important in melting with a single parameter. Nevertheless, the idea is appealing for a number of reasons.

First of all, it incorporates other previously proposed mechanisms involving defects, surfaces, and elastic properties. Since elastic constants are given by the curvature of the energy as a function of lattice strain, one would expect elastically stiff lattices to correlate with large MS barriers, and hence, high melting temperatures. Crystal instabilities at finite strain, derived in terms of elastic stiffness coefficients, have been related to the limit of metastability in the superheating of defect free crystals without surfaces.<sup>13</sup> In a finite crystal, displacements associated with lattice strain are greatest at the surface. Thus, one would expect disorder associated with strain dynamics to develop first at the surface, perhaps in the form of defects. The role of defects can be explored in the context of large strain deformation by considering a many-atom computational cell. With a large number of atoms per unit cell, the structures associated with shape change may involve defects. To illustrate this point, an MD simulation was carried out for a computational unit cell of 60 atoms interacting with the  $c_2/c_1=0.5$  potential and periodic boundary conditions. The cell shape was gradually changed, over  $\sim 16\,000$  time steps, according to the MS prescription, while maintaining a constant temperature of  $\sim 0.04$ . The results in Fig. 9 illustrate a defect-mediated shape change. After  $\sim 1600$  steps the structure (a) is basically the same as the unstrained structure except the interatomic separations are  $\sim 7\%$  longer in the  $x$  direction and  $\sim 7\%$  shorter in the  $y$  direction. After  $\sim 200$  more steps the structure becomes defective, as shown in (b). With another  $\sim 200$  steps, the defects move to create a lattice with a small orientational change from the original one. This type of adjustment to the changing cell shape happened several more times during the simulation, to produce, finally, the structure in (d). One would expect a defect-mediated shape change to be increasingly more important for systems where low MS barriers are unavailable. This could be why  $T_m$  increases initially at about the same rate as the MS barrier, on both sides of the minimum (Fig. 4), and then more gradually, compared to the MS barrier, away from the minimum.

Secondly, it places melting in the same category as many other structural phase transitions. Born’s theory of melting,<sup>14</sup> which later was considered to be a failure by most people, including Born himself,<sup>15</sup> is one of the earliest attempts to relate a structural transition to a soft mode. Subsequently, the

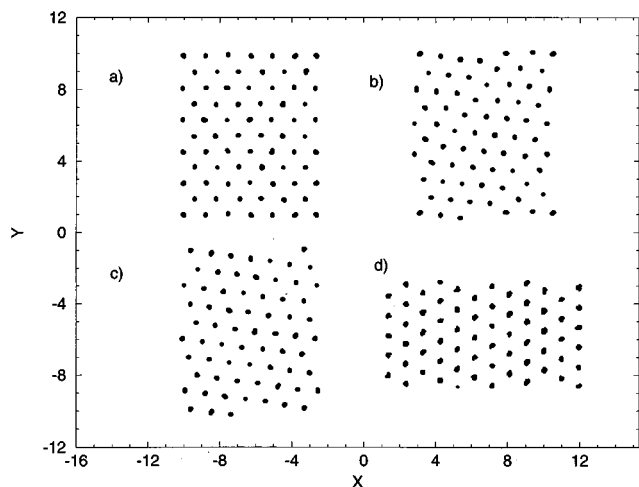


FIG. 9. Position plots for selected portions of an  $N=60$  atom bulk (computational cell with periodic boundary conditions) simulation for the  $c_2/c_1=0.5$  potential, in which the computational cell shape was gradually changed according to the MS condition, while maintaining a temperature of  $\sim 0.04$ : (a), (b), and (c) illustrating the first defect-mediated structural reconfiguration, and (d) showing the final structure.

idea was successfully applied to displacive transitions by Cochran and others.<sup>16</sup> It has become customary to think of displacive transitions as the “freezing-in” of soft modes. This is a correct picture, if it is understood that the observed mode softening results from highly anharmonic motion associated with a landscape involving energy barriers; rather than, simply, from the dynamics associated with a temperature-dependent change in a certain harmonic portion of the landscape. Clearly, the landscape associated with lattice strain, or, more generally, shape change, is a much more complicated function than that associated with a soft-mode displacive transition. Nevertheless, the principle is the same. Structural transitions occur when a system acquires enough thermal energy to overcome barriers in the energy landscape. Whether we have a displacive transition or melting, the change in structure is characterized by the barriers overcome.

Finally, it provides a distinction between the liquid and gas phases other than simply their relative densities. Specifically, a liquid is formed when a solid obtains enough thermal energy to overcome barriers associated with shape change, while a gas is formed when the thermal energy approaches the dissociation energy. In these calculations the dissociation energy was kept fixed at unity. Only potentials with low enough shape-change barriers to permit melting without evaporation in MD simulations of  $\sim 100\,000$  time steps were considered. Of course, a free cluster would always evaporate in a sufficiently long simulation.

## V. CONCLUSIONS

Simple pair potentials can be constructed which stabilize the square lattice over the hexagonal lattice in 2D. A form for such potentials, Eq. (1), has flexibility for easy adjustment to give either square or hexagonal ground states. Obviously, other functional forms could be chosen to achieve the same result. The width of the potential must be great enough to accommodate first and second neighbors of the square lattice, but not wide enough to do the same for the hexagonal lattice.

The energy of crystals as a function of small lattice strain has been widely studied theoretically in order to compare with experimentally observed elastic properties. However, there has been very little study of crystals undergoing large lattice strain. This is understandable from an experimental point of view because crystals tend to break when they are strained more than a few percent. On the other hand, accurate calculations carried out for large lattice strains provide new insights and even new metastable structures for well-known elemental systems.<sup>17,18</sup> The calculations reported here and previously (for 3D systems) suggest that the energy of crystals as a function of large lattice strains is important for determining properties of condensed matter at high temperatures.

## ACKNOWLEDGMENTS

The author is grateful for helpful discussions with J. Q. Broughton and T. Chou.

\*Work performed as visiting scholar at Harvard University.

<sup>1</sup>W. G. Hoover, D. A. Young, and R. Grover, *J. Chem. Phys.* **56**, 2207 (1972).

<sup>2</sup>J. Q. Broughton, G. H. Gilmer, and J. D. Weeks, *Phys. Rev. B* **25**, 4651 (1982).

<sup>3</sup>R. C. Gann, S. Chakravarty, and G. V. Chester, *Phys. Rev. B* **20**, 326 (1979).

<sup>4</sup>J. P. McTague, D. Frenkel, and M. P. Allen, *Ordering in Two Dimensions*, edited by S. K. Sinha (Elsevier, North-Holland, Amsterdam, 1980), p. 147.

<sup>5</sup>K. Zabinska, *Phys. Rev. B* **43**, 3450 (1991).

<sup>6</sup>A. J. C. Ladd and W. G. Hoover, *J. Chem. Phys.* **74**, 1337 (1979).

<sup>7</sup>L. L. Boyer, E. Kaxiras, M. J. Mehl, J. L. Feldman, and J. Q. Broughton, *Ordering and Disorder in Alloys*, edited by A. R. Yavari (Elsevier, Amsterdam, 1992), p. 506.

<sup>8</sup>J. Daeges, H. Gleiter, and J. H. Perepezko, *Phys. Lett. A* **119**, 79 (1986).

<sup>9</sup>J. Broughton, *Phys. Rev. Lett.* **67**, 2990 (1991).

<sup>10</sup>M. A. Glaser and N. A. Clark, *Adv. Chem. Phys.* **83**, 543 (1993).

<sup>11</sup>L. L. Boyer, E. Kaxiras, and M. J. Mehl, in *Kinetics of Phase Transformations*, edited by M. O. Thompson, M. Aziz, and G. B. Stephenson, MRS Symposia Proceedings No. 205 (Materials Research Society, Pittsburgh, 1992), p. 477.

<sup>12</sup>The term energy landscape, technically the potential energy as a general function of the atomic positions, is used here to call attention to the complex assortment of maxima, minima, saddle points, etc. (hills, valleys, ridges) that this function possesses.

<sup>13</sup>J. Wang, S. Yip, S. R. Phillpot, and Dieter Wolf, *Phys. Rev. Lett.* **71**, 4182 (1993).

<sup>14</sup>M. Born, *J. Chem. Phys.* **7**, 591 (1939).

<sup>15</sup>M. Born and K. Huang, *Dynamical Theory of Crystal Lattices* (Clarendon, Oxford, 1954), p. 413.

<sup>16</sup>W. Cochran, *Ferroelectrics* **35**, 3 (1981), and references therein.

<sup>17</sup>M. J. Mehl and L. L. Boyer, *Phys. Rev. B* **43**, 9498 (1991).

<sup>18</sup>L. L. Boyer, E. Kaxiras, J. L. Feldman, J. Q. Broughton, and M. J. Mehl, *Phys. Rev. Lett.* **67**, 715 (1991); **67**, 1477 (1991).